



Published in final edited form as:

ChemMedChem. 2010 September 3; 5(9): 1435–1438. doi:10.1002/cmdc.201000250.

Ease of Synthesis, Controllable Sizes, and In Vivo Large Animal Lymph Migration of Polymeric Nanoparticles

Ms. Kimberly Ann V. Zubris,

Departments of Biomedical Engineering and Chemistry, Boston University, Boston, MA 02215

Dr. Onkar V. Khullar,

Division of Thoracic Surgery, Department of Surgery, Brigham and Women's Hospital, Boston, MA 02215

Dr. Aaron P. Griset,

Departments of Biomedical Engineering and Chemistry, Boston University, Boston, MA 02215

Dr. Summer Gibbs-Strauss,

Division of Hematology/Oncology, Department of Medicine Beth, Israel Deaconess Medical Center, Boston, MA 02215

Dr. John V. Frangioni,

Division of Hematology/Oncology, Department of Medicine Beth, Israel Deaconess Medical Center, Boston, MA 02215

Dr. Yolonda L. Colson, and

Division of Thoracic Surgery, Department of Surgery, Brigham and Women's Hospital, Boston, MA 02215

Prof. Mark W. Grinstaff

Departments of Biomedical Engineering and Chemistry, Boston University, Boston, MA 02215

Yolonda L. Colson: ycolson@partners.org; Mark W. Grinstaff: mgrin@bu.edu

Abstract

Polymeric nanoparticles were synthesized using both a photoinduced and base-catalyzed free radical polymerization method. These mild room temperature approaches allow sensitive molecules, such as dyes, to be encapsulated. Using this method, near infrared dye loaded nanoparticles for lymphatic migration and lymph nodes localization were synthesized. After injection into a large animal, we observed migration of the nanoparticles over 20 cm to the sentinel lymph. Nanoparticle migration was observed for nanoparticles of 50 nm but not 100 nm in diameter. These investigations further support the development of new materials and clinical approaches to treat cancer including identification of nodal disease, characterization of the extent of disease, and establishment of treatment regimes.

Keywords

nanoparticles; polymerization; redox chemistry; imaging agents; drug delivery

Nanoparticles are finding ever increasing uses in a wide range of fields including photonics, catalysis and medicine, and identification of new compositions and synthetic methods is key

Correspondence to: Yolonda L. Colson, ycolson@partners.org; Mark W. Grinstaff, mgrin@bu.edu.

All animal experiments were in accordance with BIDMC IACUC approved protocol.

to the continued discoveries with these materials. Within the medical arena, nanoparticles are being investigated for drug delivery and medical imaging applications.^[1-8] Our efforts are focused on exploring synthetic procedures that will enable a greater diversity of polymer compositions, encapsulants, and sizes, and thus greater resultant nanoparticle utility. We recently reported the preparation of responsive nanoparticles from an acrylate monomer for the triggered release of paclitaxel.^[9] Here we further expand upon this synthetic approach and the use of two free radical polymerization initiation methods. Both of these mild, room temperature reactions allow for a range of monomers to be used and for control of particle size. As our interest lies in the diagnosis and treatment of lung cancer at its various stages, including metastases, we evaluated these nanoparticles for lymphatic migration in a large animal.

Nanoparticles (NPs) were prepared using a miniemulsion polymerization technique,^[10-12] which combines high-energy emulsification and free radical polymerization of an acrylate monomer and crosslinker. This is in contrast to the more common solvent evaporation method for synthesizing nanoparticles (such as for poly(lactic acid-glycolic acid) NPs),^[13-19] which uses a previously synthesized polymer. Both photoinduced and base-catalyzed reactions were explored to initiate the free radical polymerization. Specifically, nanoparticles were prepared from monomers **1-5** as shown in Figure 1. The monomers were synthesized in good to high yields (59-88%) by reacting the primary hydroxyl, secondary hydroxyl or primary amine with methacryloyl chloride or methacrylic anhydride. The complete synthetic protocols are found in the SI. These structures are representative of the diverse range of monomers that can be designed, synthesized, and used to prepare NPs with specific properties, including those monomers based on a carbohydrate (glycerol), an amino acid (serine), and a fluorescent dye (coumarin). This NP procedure is also amenable to working with a variety of common chemical linkages such as esters, amides, ethers, carbamates, and acetals which are present in our monomers.

To prepare the nanoparticles, the monomer (50 mg) and a crosslinker (1,4-*O*-methacryloylhydroquinone, **6**, 0.5 mg) were dissolved in a small amount of dichloromethane (0.5 mL). The miniemulsion was formed by adding this organic solution to an aqueous solution (2 mL) of the surfactant sodium dodecyl sulfate (SDS) and sonicating the mixture at 35 W of power for 10 minutes while under an argon blanket (Figure 2). Next, the free radical initiation system was added. When using the photochemical initiation method, eosin Y dye, 1-vinyl-2-pyrrolidinone, and triethanolamine were added to the emulsion, followed by irradiation under a Xe arc lamp for 20 minutes while being stirred. When using the base-catalyzed reaction, ammonium persulfate (APS) and *N,N,N',N'*-tetramethylethylenediamine (TEMED) were added to the emulsion while stirring under an argon blanket. Both initiation methods allow polymerization to be carried out under mild, room temperature conditions. The base-catalyzed initiation method also allows particles to be synthesized in the absence of light – critical when working with photosensitive monomers or encapsulants. Following polymerization using either method, the resultant nanoparticle suspensions were stirred overnight while open to the atmosphere to allow the remaining organic solvent to evaporate. The nanoparticles were then dialyzed against 5 mM, pH 8.0 phosphate buffer over two days to remove excess surfactant and salts. Dynamic light scattering (DLS) measurements revealed suspensions of small diameter, relatively monodisperse particles for nanoparticles prepared from monomers **1-5**. Images obtained with scanning electron microscopy (SEM) show the spherical shape and smooth morphology of particles prepared with 5 mg SDS (Figure 2, NPs composed of monomer **1**; Figure 3, NPs composed of monomers **2-4**). As shown in the micrographs, the size of the nanoparticles was dependent upon which monomer was used.

We also altered our experimental conditions to prepare nanoparticles of various sizes. As shown in Table 1, the amount of SDS used when synthesizing nanoparticles from monomer **1** was varied between 0.5 and 5 mg, thus enabling the synthesis of nanoparticles with an average diameter as large as ≈ 200 nm and as small as ≈ 50 nm, respectively. Control of NP size depends not only on the particle composition, but also on the amount of surfactant present in the aqueous phase.

Next, pyrene was encapsulated within the nanoparticles prepared from **1** as a model fluorescent molecular probe. Pyrene has an emission spectrum that contains five peaks. The relative intensities of the peak I and peak III heights can be used to measure the local hydrophilicity/hydrophobicity of the pyrene environment.^[20] Pyrene encapsulation was accomplished by adding pyrene (3% wt/wt monomer) into the organic solution of monomer while performing the miniemulsion polymerization procedure. The resulting particle suspension in water was excited at a wavelength of 321 nm, and the emission was recorded over the range of 360 – 550 nm. The encapsulated pyrene signal had a peak I/peak III ratio of 1.24, characteristic of a more hydrophobic medium than water as the peak I/peak III ratio in water is 1.96^[20], confirming entrapment of the dye within the hydrophobic nanoparticle (Figure 4).

The detection and subsequent treatment of lymph node metastases in patients is critically important for reducing morbidity and mortality.^[21-23] Significant advances have been made in the detection of lymph node metastases using nanoparticles. For example, intravenous injection of superparamagnetic iron oxide nanoparticles of 30 nm will reach the lymphatic system and be transported to the lymph nodes in animals and patients. These lymph nodes can then be imaged using magnetic resonance imaging to determine the site of metastases.^[24-26] There have also been reports using polymeric nanoparticles, and this approach offers several opportunities for lymphatic imaging and drug delivery.^[27-38] These previous studies were conducted using small animal models (such as injection into a rat footpad or mouse tail) where the migration distances are limited. For our *in vivo* lymphatic migration studies, we synthesized ≈ 50 and 120 nm diameter nanoparticles from monomer **1** and the coumarin monomer **5** (5% wt/wt monomer of **1**) loaded with the near infrared dye IR-786 (50 μ M), using the base-catalyzed method. The emission spectrum of the resulting dual-labeled NPs is shown in Figure 4. Since the λ_{max} for emission are distinct for the two dyes, we were able to perform localization studies of the NP and encapsulant. Specifically, the nanoparticles were injected subcutaneous into the breast of fully anesthetized Yorkshire pigs (n=4). The animals were imaged with a FLARE™ NIR imaging system 24 hours later using a previously described method,^[39] and only the ≈ 50 nm nanoparticles were observed to migrate. The nanoparticles migrated over 20 cm to the regional draining lymph nodes within the neck or inguinal regions. As shown in Figure 5, the near infrared color-fluorescence merged image clearly shows delivery of the fluorescent nanoparticles to the draining sentinel lymph node (SLN) from an injection site within the breast. Upon surgical removal of the sentinel lymph node and histological analysis with fluorescent microscopy,^[40] we observed co-localization of the fluorescence signals of the coumarin and IR-786 dye within the SLN confirming delivery of the IR dye via the NP (Figure 5B-D). Our study demonstrates that polymeric nanoparticles are effective at migrating over large distances, critical for eventual human use.

In summary, we have synthesized polymeric nanoparticles using a variety of monomers under mild conditions. This miniemulsion polymerization system will allow different monomers and encapsulants to be easily combined, in addition to enabling the preparation of particles of different sizes. The room temperature, mild photoinduced or base-catalyzed polymerization methods also allow sensitive molecules, such as dyes, to be encapsulated. For example, near infrared dye loaded nanoparticles for lymphatic migration and lymph

node localization were synthesized, and successfully used in a large animal model. Continued research in this area will increase our repertoire of materials and synthetic procedures available for the design of application specific nanoparticles. In the cancer arena, these investigations will facilitate the development of new approaches to identify nodal disease, characterize the extent of disease, and establish treatment regimes.

Experimental Section

Nanoparticles were prepared using a miniemulsion polymerization method where 50 mg of monomer, (**1**, **2**, **3**, **4** or **5**), and 0.5 mg of crosslinker **6** were first dissolved in 0.5 mL of CH₂Cl₂. This organic solution was then added to 2 mL of a 10 mM aqueous buffer solution containing 0.5 to 5 mg sodium dodecyl sulfate (SDS). This mixture was sonicated for 10 min (1 s pulses with a 2 s delay) with 35 W of power under an argon blanket to create the miniemulsion. When using the photochemical initiation method, following sonication, 20 μL of a 20 mM aqueous eosin Y solution and 4.27 μL of a 10% v/v aqueous 1-vinyl-2-pyrrolidinone solution were added to the emulsion. The mixture was then exposed to a xenon arc lamp (300 W) for 20 minutes while stirring to initiate polymerization. Alternatively, when using the base-catalyzed reaction, following sonication, 20 μL of a 200 mM aqueous ammonium persulfate (APS) solution and 2 μL of *N,N,N',N'*-tetramethylethylenediamine (TEMED) were added to the emulsion and stirred under an argon blanket for 2 hrs. Following polymerization using either method, the suspension was then stirred overnight while open to the atmosphere to allow the remaining solvent to evaporate. The resulting polymeric nanoparticles were then dialyzed against 5 mM pH 8.0 phosphate buffer over two days to remove excess surfactant and salts.

Acknowledgments

This work was supported in part by funds from CIMIT (MWG & YLC), BWH (YLC), and NIH grants R01-CA-115296 (JVF) and R01-EB-005805 (JVF).

References

1. Torchilin VP. *Adv Drug Deliv Rev.* 2006; 58:1532–1555. [PubMed: 17092599]
2. Davis ME, Chen Z, Shin DM. *Nature Reviews Drug Discovery.* 2008; 7:771–782.
3. Brigger I, Dubernet C, Couvreur P. *Adv Drug Deliver Rev.* 2002; 54:631–651.
4. Soppimath K. *Journal of Controlled Release.* 2001; 70:1–20. [PubMed: 11166403]
5. Gu FX, Karnik R, Wang AZ, Levy-Nissenbaum E, Hong S, Langer RS, Farokhzad OC. *Nanotoday.* 2007; 2:14–21.
6. Couvreur P, Vauthier C. *Pharm Res.* 2006; 23:1417–1450. [PubMed: 16779701]
7. Owens DE, Peppas NA. *Int J Pharm.* 2006; 307:93–102. [PubMed: 16303268]
8. Brannon-Peppas L, Blanchette JO. *Adv Drug Deliv Rev.* 2004; 56:1649–1656. [PubMed: 15350294]
9. Griset AP, Walpole J, Liu R, Gaffey A, Colson YL, Grinstaff MW. *J Am Chem Soc.* 2009; 131:2469–2471. [PubMed: 19182897]
10. Thickett SC, Gilbert RG. *Polymer.* 2007; 48:6965–6991.
11. Anton N, Benoit JP, Saulnier P. *J Cont Rel.* 2008; 128:185–199.
12. Schork FJ, Luo Y, Smulders W, Russum JP, Butte A, Fontenot K. *Adv Polym Sci.* 2005; 175:129–255.
13. Jain RA. *Biomaterials.* 2002; 21:2475–2490. [PubMed: 11055295]
14. Dong Y, Feng SS. *Int J Pharm.* 2007; 342:208–214. [PubMed: 17560058]
15. Fonseca C, Simoes S, Gaspar R. *J Control Release.* 2002; 83:273–286. [PubMed: 12363453]
16. Mo Y, Lim LY. *J Control Release.* 2005; 108:244–262. [PubMed: 16213056]
17. Panyam J, Labhasetwar V. *Adv Drug Deliv Rev.* 2003; 55:329–347. [PubMed: 12628320]

18. Sato H, Wang YM, Adachi I, Horikoshi I. *Biol Pharm Bull.* 1996; 19:1596–1601. [PubMed: 8996646]
19. Bazile DV, Ropert C, Huve P, Verrecchia T, Marlard M, Frydman A, Veillard M, Spenlehauer G. *Biomaterials.* 1992; 13:1093–1102. [PubMed: 1493193]
20. Tedeschi C, Molhwald H, Kirstein S. *J Am Chem Soc.* 2001; 123:954–960. [PubMed: 11456630]
21. Ravizzini G, Turkbey B, Barrett T, Kobayashi H, Choyke PL. *Wiley Interdisciplinary Reviews - nanomedicine and nanobiotechnology.* 2009; 1:610–623. [PubMed: 20049820]
22. Thorek DLJ, Chen A, Czupryna J, Tsourkas A. *Ann Biomed Eng.* 2006; 34:23–38. [PubMed: 16496086]
23. McCarthy JR, Kelly KA, Sun EY, Weissleder R. *Nanomed.* 2007; 2:153–167.
24. Harisinghani MG, Barentsz J, Hahn PF, Deserno WM, Tabatabaei S, van de Kaa CH, de la Rosette J, Weissleder R. *N Engl J Med.* 2003; 348:2491–U2495. [PubMed: 12815134]
25. Weissleder R, Elizondo G, Wittenberg J, Lee AS, Josephson L, Brady TJ. *Radiology.* 1990; 175:494–498. [PubMed: 2326475]
26. Rockall AG, Sohaib SA, Harisinghani MG, Babar SA, Singh N, Jeyarajah AR, Oram DH, Jacobs IJ, Shepherd IJ, Reznick RH. *J Clin Oncol.* 2005; 23:2813–2821. [PubMed: 15837995]
27. Xie Y, Bagby TR, Cohen M, Forrest ML. *Expert Opin Drug Deliv.* 2009; 6:785–792. [PubMed: 19563270]
28. Liu J, Meisner D, Kwong E, Wu XY, Johnston MR. *Cancer Res.* 2009; 69:1174–1181. [PubMed: 19176391]
29. Rao DA, Forrest ML, Alani AW, Kwon GS, Robinson JR. *J Pharm Sci.* 2009; 99:2018–2031. [PubMed: 19902520]
30. Hawley AE, Illum L, Davis SS. *FEBS Lett.* 1997; 400:319–323. [PubMed: 9009222]
31. Lu HX, Li B, Kang Y, Jiang W, Huang Q, Chen QH, Li LM, Xu CJ. *Cancer Chemother Pharmacol.* 2007; 59:175–181. [PubMed: 16718469]
32. Maincent P, Thouvenot P, Amicabile C, Hoffman M, Kreuter J, Couvreur P, Devissaguet JP. *Pharm Res.* 1992; 9:1534–1539. [PubMed: 1488394]
33. Manolova V, Flace A, Bauer M, Schwarz K, Saudan P, Bachmann MF. *Eur J Immunol.* 2008; 38:1404–1413. [PubMed: 18389478]
34. Moghimi SM. *FEBS Lett.* 2003; 540:241–244. [PubMed: 12681515]
35. Moghimi SM, Hawley AE, Christy NM, Gray T, Illum L, Davis SS. *FEBS Lett.* 1994; 344:25–30. [PubMed: 8181558]
36. Reddy ST, Rehor A, Schmoekel HG, Hubbell JA, Swartz MA. *J Cont Rel.* 2006; 112:26–34.
37. Reddy ST, van der Vlies AJ, Simeoni E, Angeli V, Randolph GJ, O'Neil CP, Lee LK, Swartz MA, Hubbell JA. *Nat Biotechnol.* 2007; 25:1159–1164. [PubMed: 17873867]
38. Nishioka Y, Yoshino H. *Adv Drug Deliv Rev.* 2001; 47:55–64. [PubMed: 11251245]
39. Troyan S, Kianzad V, Gibbs-Strauss S, Gioux S, Matsui A, Oketokoun R, Ngo L, Khamene A, Azar F, Frangioni J. *Ann Surg Oncol.* 2009; 16:2943–2952. [PubMed: 19582506]
40. Zaheer A, Lenkinski RE, Mahmood A, Jones AG, Cantley LC, Frangioni JV. *Nat Biotechnol.* 2001; 19:1148–1154. [PubMed: 11731784]

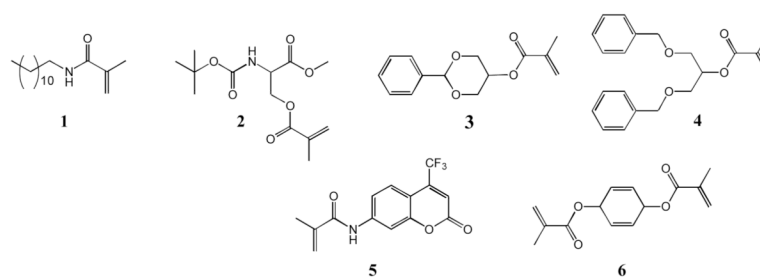


Figure 1. Chemical structures of the monomers and crosslinker used to prepare the nanoparticles.

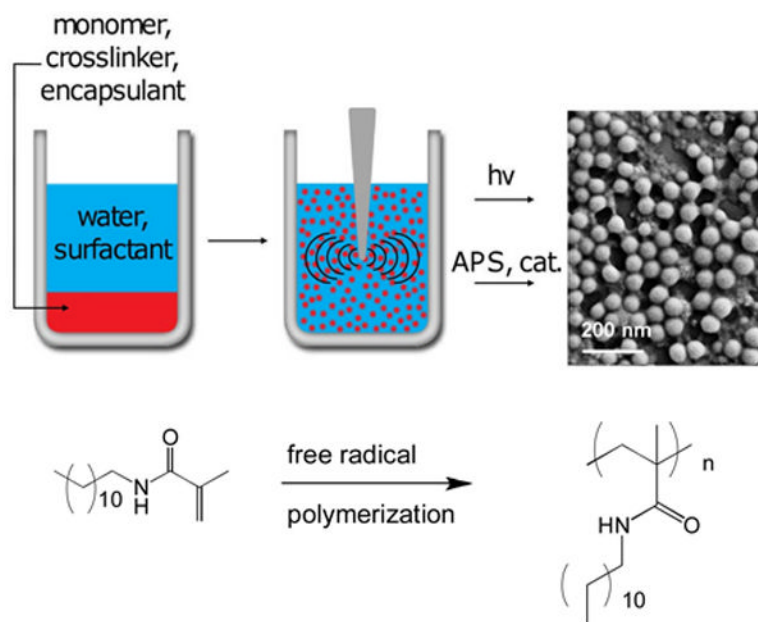


Figure 2. Scheme to synthesize the nanoparticles. The organic monomer solution is emulsified in an aqueous surfactant solution using sonication, followed by free radical polymerization.

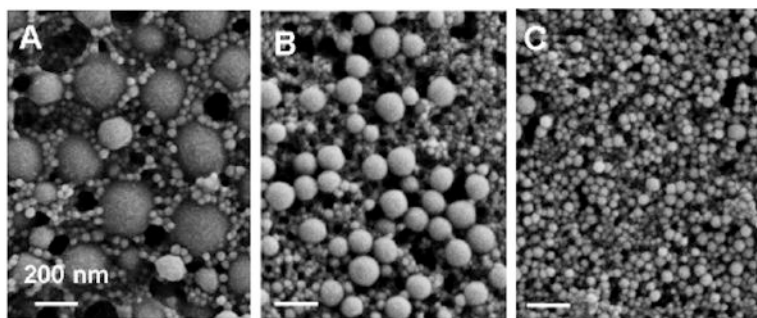


Figure 3. SEM micrographs of particles prepared from monomers **2-4**, in A-C, respectively. Scale bar = 200 nm.

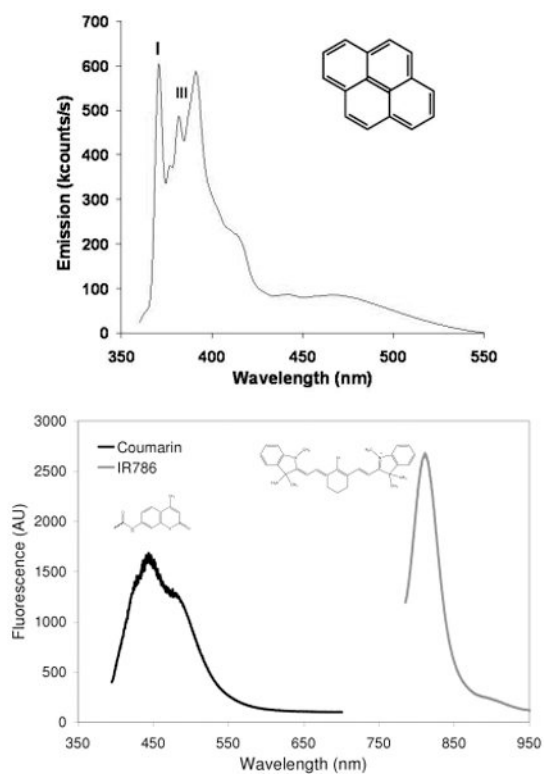


Figure 4. (top) Emission spectrum of nanoparticle encapsulated pyrene (insert) with peaks I and III denoted. (bottom) Emission spectrum of nanoparticles containing a covalently bound coumarin dye and an encapsulated near infrared dye IR-786.

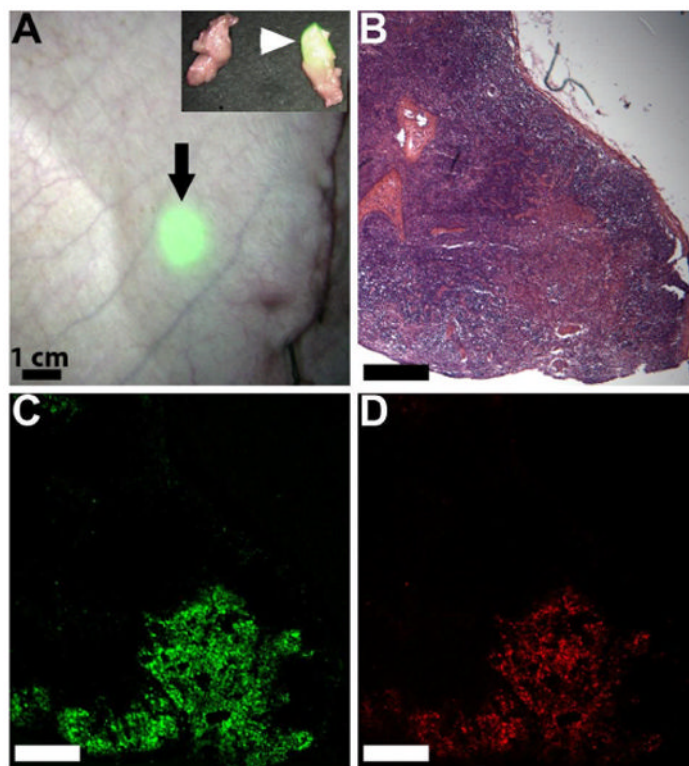


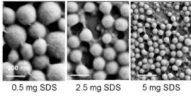
Figure 5.

(A) Visualization of the sentinel lymph node (arrow) through the skin of a live pig after injection of nanoparticles loaded with IR-786 dye into the breast (not shown). Invisible NIR fluorescent light was pseudo-colored in lime green and superimposed on the color video image to produce this merged image. The nanoparticles have localized in the lymph node 24 cm from the site of injection. The insert shows the fluorescent SLN after excision along with a non-fluorescent, negative adjacent node. (B) Histological analysis of the lymph node confirms co-localization of (C) encapsulated IR-786 and (D) coumarin-labeled NP within the SLN.

Table 1

Summary of the different sizes of nanoparticles synthesized from monomer **1** as determined by DLS and SEM.

#	SDS (mg)	Diameter (nm) via DLS	Diameter (nm) via SEM
1	0.5	215	182
2	2.5	134	110
3	5	61	40



0.5 mg SDS 2.5 mg SDS 5 mg SDS